



Published in final edited form as:

*J Phys Chem B*. 2006 October 26; 110(42): 20756–20758. doi:10.1021/jp065404d.

## Dip-Pen Nanolithography of High Melting-Temperature Molecules

Ling Huang, Yu-Hsu Chang, Joseph J. Kakkassery, and Chad A. Mirkin

Department of Chemistry and International Institute for Nanotechnology, Northwestern University, 2145 Sheridan Road, Evanston, IL 60208–3113

### Abstract

Direct nanopatterning of a number of high melting-temperature molecules have been systematically investigated by Dip-Pen Nanolithography (DPN). By tuning DPN experimental conditions, all of the high melting-temperature molecules transported smoothly from the AFM tip to the surface at room temperature without tip pre-heating. Water meniscus formation between the tip and substrate is found to play a critical role in patterning high melting-temperature molecules. These results show that heating an AFM probe to a temperature above the ink's melting temperature is not a prerequisite for ink delivery, which extends the current “ink-substrate” combinations, available to DPN users.

### Introduction

Nanostructure fabrication technologies are essential for developing and capitalizing on the emerging fields of nanoscience and nanotechnology. In particular, there is a demand for technologies that can manipulate both hard and soft materials at the sub-100 nm to many micrometer length scale.<sup>1,2</sup> Of the emerging technologies, direct-write methods are preferred because in such approaches, structures are fabricated without the use of masks, thereby allowing rapid and cost-effective prototyping. As a high resolution and high registration direct-write lithographic technology, Dip-Pen Nanolithography (DPN)<sup>3–5</sup> has been used to pattern surfaces, spanning insulating, semiconducting, and metallic substrates with a wide variety of ink materials.<sup>2</sup> Inks that have been studied thus far include: small organic molecules,<sup>6–10</sup> organic macromolecules,<sup>11,12</sup> sol gels,<sup>13</sup> biopolymers<sup>14</sup> and proteins.<sup>15</sup> Templates made by DPN have been used for studying polymer crystallization,<sup>16</sup> individual virus particles,<sup>17</sup> biorecognition,<sup>18–20</sup> and optical and electrical transport in a wide variety of nanostructures.<sup>21,22</sup>

The relative humidity and the meniscus that forms at the point of contact between the AFM tip and substrate have been used to regulate the ink transport process.<sup>23</sup> However, many of the molecules that have been studied thus far (e.g. 1-octadecanethiol (ODT) and 16-mercaptohexadecanoic acid (MHA)) have melting points close to room temperature bringing into question the role of vapor transport. Indeed, others have studied certain higher melting point molecules such as octadecylphosphonic acid (OPA) and concluded that the DPN deposition process only occurs when the cantilever tip is heated above the molecule's melting point.<sup>24</sup> However, in previous studies we found that a variety of high melting temperature materials such as DNA transport rapidly at room temperature under the appropriate humidity.<sup>14</sup> Our understanding of the role of the meniscus and water solvation of the molecules coating the tip suggests that as long as a compound has some solubility in water it should transport regardless of its melting temperature.<sup>23</sup> Herein, we explore the transport properties of a variety

Email: chadnano@northwestern.edu Tel: 847.467.7302 Fax: 847.467.5123.

**Supporting Information Available:** Height profiles of DPN generated line arrays shown in Figure 1B and Figure 4. This material is available free of charge via the Internet at <http://pubs.acs.org>.

of high melting point molecules, including OPA, in the context of a DPN experiment (Table 1) and show that they all can be transported effectively to form stable nanostructures, providing the appropriate humidity is used in all cases.

## Experimental Section

2-Mercaptobenzothiazole (2MBT), 4-amino-5-hydrazino-1,2,4-triazole-3-thiol (Purpald), 4-mercaptopyridine (4MP), and 2-mercaptoimidazole (2MI) were purchased from Sigma Aldrich (Milwaukee, WI), and octadecylphosphonic acid (OPA) was purchased from Alfa Aesar (Ward Hill, MA). Ethanol was ordered from Fisher Scientific, and all of the compounds and solvents were used as received. A saturated solution of Purpald in ethanol and 1 mM ethanol solutions of 2MBT, 4MP, OPA, and 2MI were used, respectively, for tip-coating in all DPN experiments. The solubility of each compound was determined by the amount of compound that would dissolve in 20 ml of water at room temperature.

DPN of OPA was performed at 45% relative humidity at room temperature. For all other thiol containing molecules, the relative humidity was maintained at  $85 \pm 5\%$  during the DPN process, and the temperature fluctuated between 25.0 to 29.0 °C, which is a consequence of the hot water vapor used for humidity control.

Si/SiO<sub>x</sub> (100) wafers with 500 nm oxide coating layer were purchased from WaferNet, Inc. (San Jose, CA). Gold substrates were obtained by thermal evaporation of a gold thin film (30 nm) on a Si/SiO<sub>x</sub> substrate pre-coated with a Ti adhesion layer (7 nm).

All AFM data were obtained with a ThermoMicroscopes CP (Veeco Instruments Inc., CA) AFM, enclosed in a humidity control chamber and driven by commercially available DPN software (Nanoink Inc., Chicago, IL). (AFM probes were purchased from Nanoink Inc., either S-1 or S-2 type, with spring constants of 0.041 N/m and 0.1 N/m, respectively).

## Results and Discussion

Five compounds with melting points between 99 and 230 °C were selected as “ink” candidates for this study (Table 1). All but OPA have thiol moieties and form chemically adsorbed monolayers on gold surfaces. OPA adsorbs onto oxide surfaces and can be used to modify silicon oxide,<sup>25</sup> mica,<sup>26</sup> and indium tin oxide (ITO).<sup>27</sup> Collectively, these molecules form a representative class of adsorbates to study the importance, or lack thereof, of melting temperature on the DPN transport process.

Significantly, OPA transports readily at 45% humidity, even at 22 °C. Transport studies of OPA on SiO<sub>x</sub> show the feature size dependence on tip-substrate contact time, typically observed with conventional low melting point inks (Figure 1A). In general, the dot diameter increases with longer contact times (*t*) and exhibits a linear  $t^{1/2}$  dependence (Figure 2), which is in agreement with the meniscus-based ink transport mechanism.<sup>23,28</sup> Line patterns of OPA also could be easily obtained under similar conditions, with increasing line-widths observed at decreased writing speeds (Figure 1B).

Further studies showed that all of the four thiol containing molecules readily transport to gold substrates at room temperature (temperature variation is between 25.0 and 29.0 °C) when the experiments are carried out at  $85 \pm 5\%$  humidity, Figure 3. As with OPA, a linear  $t^{1/2}$  dependence of dot diameter to tip-substrate contact time is also observed for the selected thiol containing compounds (Figure 2), however, the required contact times to generate a specific feature size varied from molecule to molecule. This difference, in part, can be attributed to the differences in solubility of the molecules in water (Table 1) and their respective diffusion coefficients, which significantly affect their transport rate.

From the data in Figure 2 and Table 1, it is clear that there is a much greater dependence on ink solubility in water rather than on ink melting temperature with respect to transport rate. 2MI has the highest transport rate (99.3 nm/sec<sup>1/2</sup>), while Purpald has the lowest transport rate (29.4 nm/sec<sup>1/2</sup>), which is consistent with their water solubilities (Table 1). There is no obvious relationship between ink transport rate and melting temperature. For example, 2MI and Purpald have similar melting temperatures (230 °C), but their transport rates as inks are dramatically different. The transport properties of the other inks are consistent with these observations.

To further evaluate the similarity between high melting point inks and their lower melting point analogues, we generated more complex patterns such as lines with all of the inks listed in Table 1 (Figure 4). The data clearly show that all of the molecules can be easily deposited under the optimized conditions in a highly controllable fashion. As with DPN of conventional lower melting point compounds, in all cases, line width decreases with increased writing speed. The data reported here are consistent with the previously reported water meniscus mechanism,<sup>23, 28</sup> and *inconsistent* with the vapor transfer mechanism and the hypothesis that one must exceed the melting temperature of the ink to facilitate its transport.<sup>24</sup>

## Conclusions

In summary, in contrast with previous reports,<sup>24</sup> we have demonstrated that high melting point inks can be easily patterned by conventional DPN, at the appropriate humidity. Indeed, we have shown that heating of an ink to its melting point is not a prerequisite for DPN patterning. Thermal DPN may be important for inks that do not have appreciable water solubilities (e.g. metals below their melting points), but not essential for high melting point compounds. This work expands the scope of the inks that can be used in a DPN experiment and provides further evidence for the importance of water and the meniscus in the DPN transport mechanism.

## Supplementary Material

Refer to Web version on PubMed Central for supplementary material.

## Acknowledgement

This work was supported by the AFOSR, DARPA, and NSF through a NSEC. CAM is grateful for a NIH Director's Pioneer Award. JJK is thankful to the Swiss National Science Foundation for a postdoctoral fellowship.

## References and Notes

1. Gates BD, Xu QB, Stewart M, Ryan D, Willson CG, Whitesides GM. *Chem. Rev* 2005;105:1171. [PubMed: 15826012]
2. Ginger DS, Zhang H, Mirkin CA. *Angew. Chem. Int. Ed* 2004;43:30.
3. Piner RD, Zhu J, Xu F, Hong S, Mirkin CA. *Science* 1999;283:661. [PubMed: 9924019]
4. Hong S, Mirkin CA. *Science* 1999;286:523. [PubMed: 10521346]
5. Hong S, Mirkin CA. *Science* 2000;288:1808. [PubMed: 10846159]
6. Demers LM, Mirkin CA. *Angew. Chem. Int. Ed* 2001;40:3069.
7. Valiokas R, Vaitekonis A, Klenkar G, Trinkunas G, Liedberg B. *Langmuir* 2006;22:3456. [PubMed: 16584209]
8. Ivanisevic A, Mirkin CA. *J. Am. Chem. Soc* 2001;123:7887. [PubMed: 11493062]
9. Chi YS, Choi IS. *Adv. Func. Mater* 2006;16:1031.
10. Sheu JT, Wu CH, Chao TS. *J. J. Appl. Phys* 2006;45:3693.
11. Lim JH, Mirkin CA. *Adv. Mater* 2002;14:1474.
12. Maynor B, Filocamo S, Grinstaff M, Liu J. *J. Am. Chem. Soc* 2002;124:522. [PubMed: 11804474]
13. Fu L, Liu XG, Zhang Y, Dravid VP, Mirkin CA. *Nano Lett* 2003;3:757.

14. Demers LM, Ginger DS, Park SJ, Li Z, Chung SW, Mirkin CA. *Science* 2002;296:1836. [PubMed: 12052950]
15. Lee KB, Park SJ, Mirkin CA, Smith JC, Mrksich M. *Science* 2002;295:1702. [PubMed: 11834780]
16. Liu X, Zhang Y, Goswami DK, Okasinski JS, Salaita K, Sun P, Bedzyk MJ, Mirkin CA. *Science* 2005;307:1763. [PubMed: 15774755]
17. Vega RA, MasPOCH D, Salaita K, Mirkin CA. *Angew. Chem. Int. Ed* 2005;44:6013.
18. Demers LM, Park SJ, Taton TA, Li Z, Mirkin CA. *Angew. Chem. Int. Ed* 2001;40:3071.
19. Lee SW, Oh BK, Sanedrin RG, Salaita K, Fujigaya T, Mirkin CA. *Adv. Mater* 2006;18:1133.
20. Lee M, Kang DK, Yang HK, Park KH, Choe SY, Kang C, Chang SI, Han MH, Kang IC. *Proteomics* 2006;6:1094. [PubMed: 16429461]
21. Qin L, Park S, Huang L, Mirkin CA. *Science* 2005;309:113. [PubMed: 15994551]
22. Basnar B, Weizmann Y, Cheglakov Z, Willner I. *Adv. Mater* 2006;18:713.
23. Manandhar P, Jang J, Schatz GC, Ratner MA, Hong S. *Phys. Rev. Lett* 2003;90:1155051.
24. Sheehan PE, Whitman LJ, King WP, Nelson BA. *Appl. Phys. Lett* 2004;85:1589.
25. Hanson EL, Schwartz J, Nickel B, Koch N, Danisman MF. *J. Am. Chem. Soc* 2003;125:16074. [PubMed: 14677999]
26. Woodward JT, Ulman A, Schwartz DK. *Langmuir* 1996;12:3626.
27. Gawalt ES, Avaltroni MJ, Koch N, Schwartz J. *Langmuir* 2001;17:5736.
28. Cho N, Ryu S, Kim B, Schatz GC, Hong S. *J. Chem. Phys* 2006;124:024714. [PubMed: 16422633]

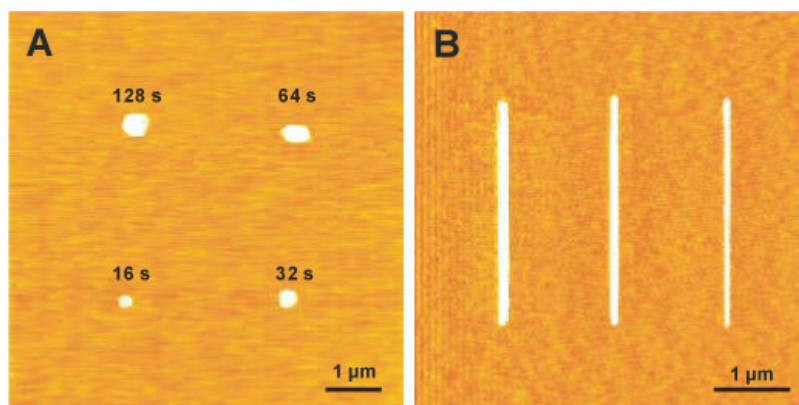


**Figure 1.** Topography AFM images of DPN-generated OPA nanopatterns on a SiO<sub>x</sub> surface. (A) Dot patterns of OPA generated at contact times of 128, 64, 32, and 16 sec. (B) Line patterns of OPA generated at writing speeds of 0.04, 0.16, and 0.64 μm/sec (from left to right).

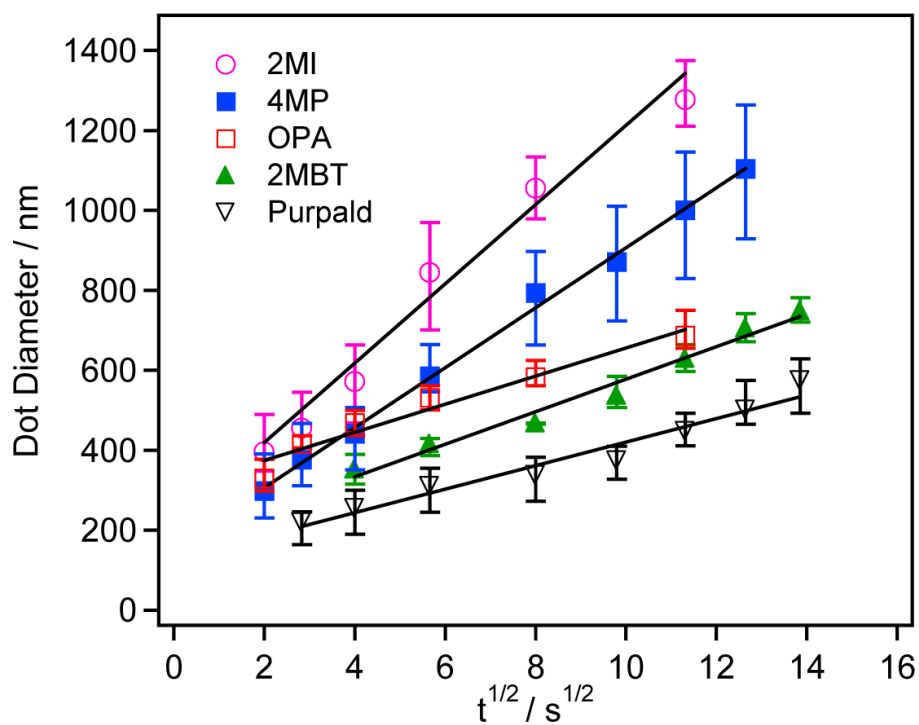


**Figure 2.** The dot diameters of OPA, 2MI, 4MP, Purpald, and 2MBT plotted as a function of the tip-substrate contact time ( $t^{1/2}$ ).

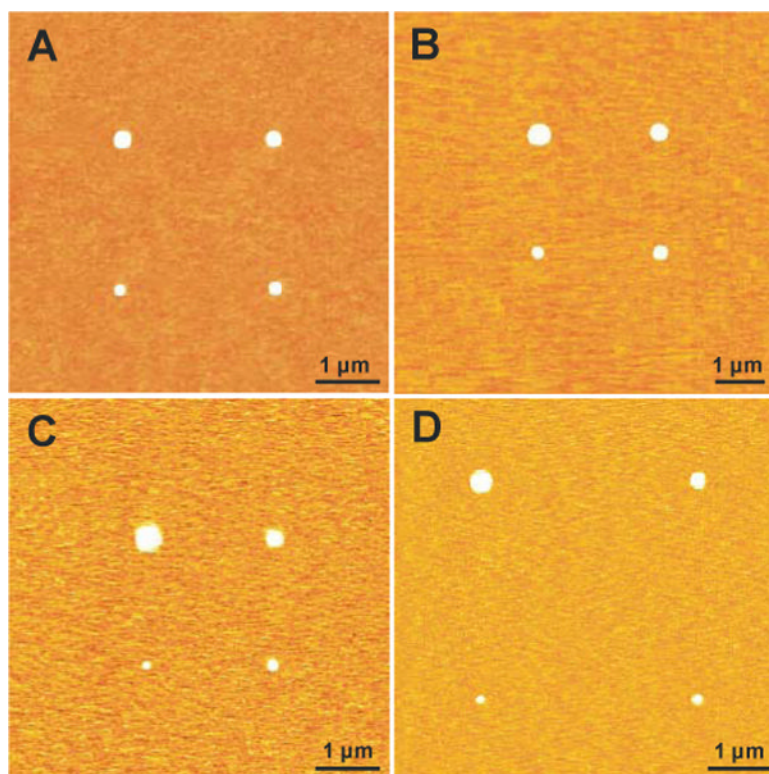


**Figure 3.** Topography AFM images of DPN-generated dot nanopatterns of (A) 2MBT at contact time of 128, 64, 32, and 16 sec; (B) Purpald at contact time of 128, 64, 32, and 16 sec; (C) 4MP at contact time of 32, 16, 8, and 4 sec, and (D) 2MI at contact time of 32, 16, 8, and 4 sec. The humidity was  $85 \pm 5\%$ , and the temperature was maintained between 25 and 29 °C.

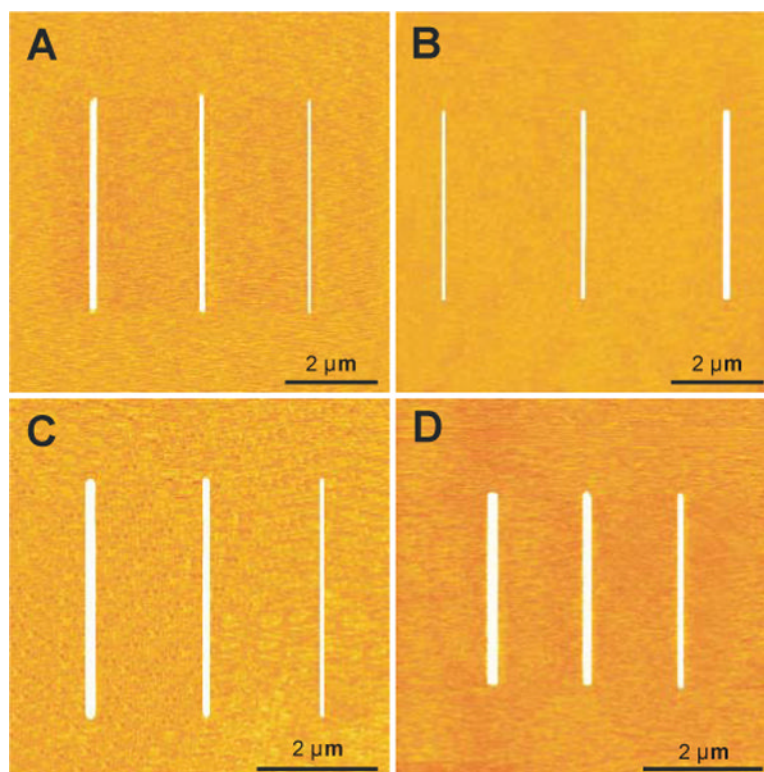


**Figure 4.** Topography AFM images of DPN line arrays of (A) 2MBT generated at writing speeds of: 0.1, 0.2, and 0.3  $\mu\text{m}/\text{sec}$  (from left to right); (B) Purpald generated at writing speeds of: 0.08, 0.04, and 0.02  $\mu\text{m}/\text{sec}$  (from left to right); (C) 4MP generated at writing speeds of: 0.1, 0.2, and 0.4  $\mu\text{m}/\text{sec}$  (from left to right), and (D) 2MI generated at writing speeds of: 0.05, 0.1, and 0.2  $\mu\text{m}/\text{sec}$  (from left to right). The humidity was  $85 \pm 5\%$ , and the temperature was maintained between 25 and 29  $^{\circ}\text{C}$ .

**Table 1**

Melting point, room temperature water solubility, and transport rate data for the DPN 'inks' studied.

	Melting Point (°C)	Solubility in Water (mg/ml)	Transport Rate (nm/sec <sup>1/2</sup> )
octadecylphosphonic acid (OPA)	99	<0.1	35.2
2-mercaptobenzothiazole (2MBT)	179~182	<0.5	40.6
4-amino-5-hydrazino-1,2,4-triazole-3-thiol (Purpald)	228~230	<0.05	29.4
4-mercaptopyridine (4MP)	177	>30	74.9
2-mercaptoimidazole (2MI)	228~231	>40	99.3